Structure and Thermal Reactivity of a Novel Pd(0) Metalloenediyne

Nicole L. Coalter,[†] Thomas E. Concolino,[‡] William E. Streib,[†] Chris G. Hughes,[†] Arnold L. Rheingold,[‡] and Jeffrey M. Zaleski*[,†]

Contribution from the Department of Chemistry, Indiana University, Bloomington, Indiana 47405, and Department of Chemistry and Biochemistry, University of Delaware, Newark, Delaware 19716

Received December 17, 1999

Abstract: We report the X-ray diffraction structure and thermal reactivity of the metalloenediyne compound bis(1,2-bis(diphenylphosphinoethynyl)benzene)palladium(0) (Pd(dppeb)$_2$, **1**). The structure of **1** features a tetrahedral Pd(0) center with four phosphorus atoms from two chelating ligands. The P—Pd—P bond angles nearly match the idealized 109.5° geometry expected for a d^{10} metal center in a tetrahedral ligand field. The tetrahedral geometry of the metal center forces the alkyne termini separation of the enediyne ligand to a distance of 3.47 Å, which results in a thermally stable compound at room temperature. However, at 115 °C **1** exhibits solvent-dependent reactivity. In *o*-fluorotoluene, **1** decomposes via ligand dissociation, while in *o*-dichlorobenzene, carbon−halide bond activation of solvent occurs leading to the oxidative addition product *trans*-Pd((2-chlorophenyl)diphenylphosphine)$_2$Cl$_2$ and free (2-chlorophenyl)diphenylphosphine. The thermal reactivity of **1** is markedly more endothermic (44 kcal/mol) than that of the known Pd(dppeb)Cl$_2$ analogue (12.3 kcal/mol). The diminished reactivity can be attributed to two factors: the increased alkyne termini separation in **1** (3.47 vs 3.3 Å) due to the metal-mandated tetrahedral geometry of the Pd(0) center, and the resistance of the Pd(0) to adopting a planar transition state geometry to promote Bergman cyclization. Overall this study demonstrates that metal binding can impose structural consequences upon the enediyne ligand governed by the oxidation state and corresponding ligand field geometry of the metal center.

Introduction

The discoveries of the unique structural motifs[1−3] and striking antitumor activities of the enediyne antibiotics have spawned extensive interest in the mechanisms[4−25] of these intriguing molecules.[26] The key feature of these natural products is the 1,5-diyne-3-ene unit that undergoes Bergman cyclization to form the potent 1,4-phenyl diradical intermediate[27,28] in the presence of biological reducing equivalents. The singlet diradical intermediate is proposed to be the species responsible for the DNA-cleaving activity of the enediynes,[29] which occurs via H-atom abstraction from the deoxyribose ring of the DNA backbone.[30] Ironically, it is this inherently facile reactivity that promotes toxicity problems in the pharmacological applications of these compounds.

* To whom correspondence should be addressed. E-mail: zaleski@indiana.edu.

† Indiana University.

‡ University of Delaware.

(1) Lee, M. D.; Dunne, T. S.; Chang, C. C.; Siegal, M. M.; Morton, G. O.; Ellestad, G. A.; McGahren, W. J.; Borders, D. B. *J. Am. Chem. Soc.* **1992**, *114*, 985.

(2) Golik, J.; Clardy, J.; Dubay, G.; Greoenewold, G.; Kawaguchi, H.; Konishi, M.; Krishnan, B.; Ohkuma, H.; Saitoh, K.; Doyle, T. W. *J. Am. Chem. Soc.* **1987**, *109*, 3461.

(3) Golik, J.; Clardy, J.; Dubay, G.; Greoenewold, G.; Kawaguchi, H.; Konishi, M.; Krishnan, B.; Ohkuma, H.; Saitoh, K.; Doyle, T. W. *J. Am. Chem. Soc.* **1987**, *109*, 3462.

(4) Takahashi, T.; Tanaka, H.; Yamada, H.; Matsumoto, T.; Sugiura, Y. *Angew. Chem., Int. Ed. Engl.* **1996**, *35*, 1835.

(5) Nicolaou, K. C.; Smith, A. L.; Wenderborn, S. V.; Hwang, C.-K. *J. Am. Chem. Soc.* **1991**, *113*, 3106.

(6) Nicolaou, K. C.; Dai, W.-M.; Wendeborn, S. V.; Smith, A. L.; Torisawa, Y.; Maligres, P.; Hwang, C.-K. *Angew. Chem., Int. Ed. Engl.* **1991**, *30*, 1032.

(7) Nicolaou, K. C.; Zuccarello, G.; Riemer, C.; Estevez, V. A.; Dai, W.-M. *J. Am. Chem. Soc.* **1992**, *114*, 7360.

(8) Nicolaou, K. C.; Ogawa, Y.; Zuccarello, G.; Kataoke, H. *J. Am. Chem. Soc.* **1988**, *110*, 7247.

(9) Zein, N.; Sinha, A. M.; McGahren, W. J.; Ellestad, G. A. *Science* **1988**, *240*, 1198−1201.

(10) Lee, M. D.; Dunne, T. S.; Siegal, M. M.; Chang, C. C.; Morton, G. O.; Borders, D. B. *J. Am. Chem. Soc.* **1987**, *109*, 3464.

(11) Lee, M. D.; Dunne, T. S.; Chang, C. C.; Ellestad, G. A.; Siegal, M. M.; Morton, G. O.; McGahren, W. J.; Borders, D. B. *J. Am. Chem. Soc.* **1987**, *109*, 3466.

(12) Aiyar, J.; Danishefsky, S. J.; Crothers, D. M. *J. Am. Chem. Soc.* **1992**, *114*, 7552.

(13) Aiyar, J.; Hitchcock, S. A.; Denhart, D.; Liu, K. K. C.; Danishefsky, S. J.; Crothers, D. M. *Angew. Chem., Int. Ed. Engl.* **1994**, *33*, 855.

(14) Drak, J.; Iwasawa, N.; Danishefsky, S.; Crothers, D. M. *Proc. Natl. Acad. Sci. U.S.A.* **1991**, *88*, 7464.

(15) Depew, K. M.; Zeman, S. M.; Boyer, S. H.; Denhart, D. J.; Ikemoto, N.; Danishefsky, S. J.; Crothers, D. M. *Angew. Chem., Int. Ed. Engl.* **1996**, *35*, 2797.

(16) Nicolaou, K. C.; Tsay, S.-C.; Suzuki, T.; Joyce, G. F. *J. Am. Chem. Soc.* **1992**, *114*, 7555.

(17) Nicolaou, K. C.; Smith, A. L. *Acc. Chem. Res.* **1992**, *25*, 497.

(18) Walker, S.; Landovitz, R.; Ding, W. D.; Ellestad, G. A.; Kahne, D. *Proc. Natl. Acad. Sci. U.S.A.* **1992**, *89*, 4608.

(19) Li, H.; Zeng, Z.; Estevez, V. A.; Baldenius, K. U.; Nicolaou, K. C.; Joyce, G. F. *J. Am. Chem. Soc.* **1994**, *116*, 3709.

(20) Liu, C.; Smith, B. M.; Ajito, K.; Komatsu, H.; Gomez-Paloma, L.; Li, T.; Theodorakis, E. A.; Nicolaou, K. C.; Vogt, P. K. *Proc. Natl. Acad. Sci. U.S.A.* **1996**, *93*, 940.

(21) Nicolaou, K. C.; Li, T.; Nakada, M.; Hummel, C. W.; Hiatt, A.; Wrasidlo, W. *Angew. Chem., Int. Ed. Engl.* **1994**, *33*, 183.

(22) Ho, S. N.; Boyer, S. H.; Schreiber, S. L.; Danishefsky, S. J.; Crabtree, R. G. *Proc. Natl. Acad. Sci. U.S.A.* **1994**, *91*, 9203.

(23) Shair, M. D.; Yoon, T.; Chou, T. C.; Danishefsky, S. J. *Angew. Chem., Int. Ed. Engl.* **1994**, *33*, 2477.

(24) Nicolaou, K. C.; Smith, B. M.; Ajito, K.; Komatsu, H.; Gomez-Paloma, L.; Tor, Y. *J. Am. Chem. Soc.* **1996**, *118*, 2303.

(25) Nicolaou, K. C.; Dai, W.-M. *Angew. Chem., Int. Ed. Engl.* **1991**, *30*, 1387.

(26) Smith, A. L.; Nicolaou, K. C. *J. Med. Chem.* **1996**, *39*, 2103.

(27) Jones, R.; Bergman, R. G. *J. Am. Chem. Soc.* **1972**, *94*, 660.

(28) Bergman, R. G. *Acc. Chem. Res.* **1973**, *6*, 25.

(29) Schreiner, P. R. *J. Am. Chem. Soc.* **1998**, *120*, 4184.

(30) Paloma, L. G.; Smith, J. A.; Chazin, W. J.; Nicolaou, K. C. *J. Am. Chem. Soc.* **1994**, *116*, 3697.

10.1021/ja9944094 CCC: $19.00
Published on Web 03/17/2000

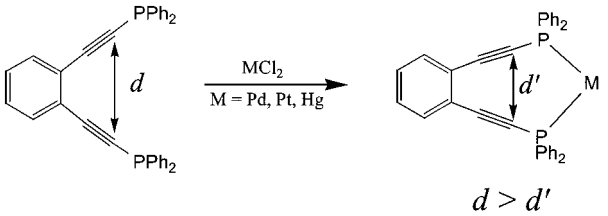

Figure 1. Modulation of the distance (*d*) between alkyne termini of the dppeb ligand by chelation to transition metal centers.

The ability to control formation of 1,4-phenyl diradical intermediates characteristic of the enediyne antitumor antibiotics[26,31] leads to the potential for designing novel compounds with pharmacological utility. To this end, a number of unique synthetic,[32,33] photochemical,[6,34−38] and electrochemical[35] approaches have been explored to initiate Bergman cyclization of organic enediynes in a controlled manner. One of the prominent themes to emerge from the original synthetic work was the empirical correlation between the alkyne termini separation distance (d = 3.2−3.31 Å, Figure 1) and the temperature for thermal cyclization.[7] Correlation of activation energies for Bergman cyclization with crystallographically determined alkyne termini distances has shown in contrast no direct relationship between distance and activation energy.[39−43] Rather, differential molecular ring strain in the ground and transition states is proposed to be the dominant contribution to the thermal barrier height for cyclic enediyne systems. More recent computational studies have confirmed the absence of an exclusive relationship between alkyne termini separation and activation enthalpy, and suggest that ring strain contributions to the thermal barrier are indeed important to Bergman cyclization reactivity.[29] However, ring strain is not the sole factor in determining the activation barrier. Density functional results also suggest that if structural perturbations were to reduce *d* to 2.9−3.4 Å, cyclization should occur spontaneously (i.e. room temperature or below) baring very large olefin ring strain.[29,44] Thus, although *d* may not be the exclusive contributor to the reaction coordinate, it appears to play a more coarsely defined supporting role in affecting enediyne cyclization temperatures.

Recently, Buchwald *et al.* have shown that chelation of the metal binding enediyne 1,2-bis(diphenylphosphinoethynyl)-benzene (dppeb) to Pd^{2+}, Pt^{2+}, and Hg^{2+} can modulate the critical distance by using the metal as a scaffold to poise the alkyne termini at a distance governed by the atomic radius of the ion (Figure 1).[45] Since this seminal work, remarkably few examples of metal-assisted thermal enediyne cyclizations have been reported[46,47] to document the utility of transition metals for affecting enediyne cyclizations. Within this theme, our efforts have focused on preparing and structurally characterizing metalloenediynes to investigate the limits to which enediyne cyclization can be modulated and controlled. We are specifically interested in determining the role of the metal center oxidation state and geometry in governing enediyne ligand disposition and the activation energy for Bergman cyclization. To date, no studies have been published comparing and contrasting the effects of metal center oxidation state and geometry on enediyne cyclization temperatures. Moreover, no crystallographic structures of enediyne ligands chelated to transition metals have been elucidated to correlate detailed geometric features with thermal Bergman cyclization reactivities.[48]

Herein we report the X-ray diffraction crystal structure and thermal reactivity of a mononuclear Pd(0) metalloenediyne compound with two chelating 1,2-bis(diphenylphosphinoethynyl)benzene ligands (dppeb). The structure is the first example of a metal-chelated enediyne compound and in conjunction with its thermal reactivity serves as a key model for understanding the factors that control metal-assisted Bergman cyclization reactions.

Experimental Section

Materials. 1,2-Bis(diphenylphosphinoethynyl)benzene was prepared according to a literature procedure. $Pd(dppeb)_2$ was prepared according to a modified literature procedure for $Pd(dppm)_3$. $Pd(PPh_3)_2Cl_2$, $Pd(CH_3CN)_2Cl_2$, and $Pd(CH_3CN)_4BF_4$ were purchased from Strem and used as received. All solvents were dried and distilled according to standard procedure except *o*-dichlorobenzene which was dried over 4 Å sieves prior to use. 1,4-Cyclohexadiene was purchase from Aldrich and used as received.

Physical Measurements. A nitrogen atmosphere drybox was used for all air-sensitive manipulations. ^1H, $^{13}C\{^1H\}$, and $^{31}P\{^1H\}$ studies were performed on a Varian Unity I400 spectrometer. ^1H and $^{13}C\{^1H\}$ spectra were referenced to the residual proton signal of the solvent, while $^{31}P\{^1H\}$ spectra were referenced with an 85% phosphoric acid standard. Differential Scanning Calorimetry (DSC) measurements were made on a TGA 910 DSC system with a TA Instruments thermal analyzer. Samples of $Pd(dppeb)_2$ were scanned at a rate of 10 °C min^{-1}.

Synthesis of $Pd(dppeb)_2$ (1). dppeb (5 g, 0.01 mol) in 10 mL of benzene was added to 3.55 g (0.005 mol) of $Pd(PPh_3)_2Cl_2$ in 50 mL of benzene. The solution was heated and stirred at 60 °C until dissolution (16 h). Without cooling, hydrazine was added dropwise until the evolution of gas ceased, resulting in a red solution with an orange precipitate. The solvent was removed in vacuo, and then the residue was dissolved in a minimum amount of CH_2Cl_2 (10 mL) and reprecipitated in cold ethanol (50 mL). The solution was filtered, and the solid collected and dried (yield: 50%). Crystals for X-ray diffraction were grown from slow evaporation of CH_2Cl_2.^1H NMR (CD_2Cl_2): δ 7.5−7.4 (m, 4H), 7.3 (br S, 16H), 7.0 (t, 8H), 6.8 (t, 16H). $^{31}P\{^1H\}$ NMR (CD_2Cl_2): δ −5.6. $^{13}C\{^1H\}$ NMR (CD_2Cl_2): δ 138.9, 134.0 (d, 20 Hz), 132.1, 130.3, 128.9 (d, 18 Hz), 128.0, 127.3, 109.1, 96.5 (d, 9 Hz).

Crystallographic Structure Determination for 1. A suitable crystal of **1** was mounted with silicone grease, transferred to a goniostat, and cooled to 105 K for data collection. A preliminary search for peaks followed by analysis using programs DIRAX and TRACER revealed

(31) Nicolau, K. C.; Dai, W.-M. *Angew. Chem., Int. Ed. Engl.* **1991**, *30*, 1387.
(32) Nicolaou, K. C.; Smith, A. L.; Yue, E. W. *Proc. Natl. Acad. Sci., U.S.A.* **1993**, *90*, 5881.
(33) Maier, M. E. *Synlett* **1995**, 13.
(34) Wender, P. A.; Zercher, C. K.; Beckham, S.; Haubold, E.-M. *J. Org. Chem.* **1993**, *58*, 5867.
(35) Ramkumar, D.; Kalpana, M.; Varghese, B.; Sankararaman, S. *J. Org. Chem.* **1996**, *61*, 2247.
(36) Funk, R. L.; Young, E. R. R.; Williams, R. M.; Flanagan, M. F.; Cecil, T. L. *J. Am. Chem. Soc.* **1996**, *118*, 3291.
(37) Turro, N. J.; Evenzahav, A.; Nicolaou, K. C. *Tetrahedron Lett.* **1994**, *35*, 8089.
(38) Evenzahav, A.; Turro, N. J. *J. Am. Chem. Soc.* **1998**, *120*, 1835.
(39) Magnus, P. J.; Carter, P. A. *J. Am. Chem. Soc.* **1988**, *110*, 1626.
(40) Magnus, P.; Lewis, R. T.; Huffman, J. C. *J. Am. Chem. Soc.* **1988**, *110*, 6921.
(41) Magnus, P.; Fortt, S.; Pitterna, T.; Snyder, J. P. *J. Am. Chem. Soc.* **1990**, *112*, 4986.
(42) Snyder, J. P. *J. Am. Chem. Soc.* **1990**, *112*, 5367.
(43) Snyder, J. P. *J. Am. Chem. Soc.* **1989**, *111*, 7630.
(44) Nantz, M. H.; Moss, D. K.; Spence, J. D.; Olmstead, M. M. *Angew. Chem., Int. Ed. Engl.* **1998**, *110*, 470.
(45) Warner, B. P.; Millar, S. P.; Broene, R. D.; Buchwald, S. L. *Science* **1995**, *269*, 814.
(46) Konig, B.; Pitsch, W.; Thondorf, I. *J. Org. Chem.* **1996**, *61*, 5258.
(47) Basak, A.; Shain, J. C. *Tetrahedron Lett.* **1998**, *39*, 3029.
(48) A search of the Cambridge Structure Database revealed no metalloenediyne structures with chelating enediyne ligands. The closest structural analogues known are the π-complexed Os(II) metal−enediyne *trans*-$[Os(en)_2(\eta^2\text{-L})Br]^+Br^-$, L = *cis*-1,6-bistrimethylsilyl-3-ene-1,5-diyne (Hasegawa, T.; Pu, L. *J. Orgmet. Chem.* **1997**, *527*, 287), and a bridging Pd(II) bisacetylide $Pd_2L(PR_3)_4Cl_2$, L = *o*-diethynylbenzene (Onitsuka, K.; Yamamoto, S.; Takahashi, S. *Angew. Chem., Int. Ed. Engl.* **1999**, *38*, 174).

Scheme 1. Synthesis and Solid State Thermal Reactivity of **1**

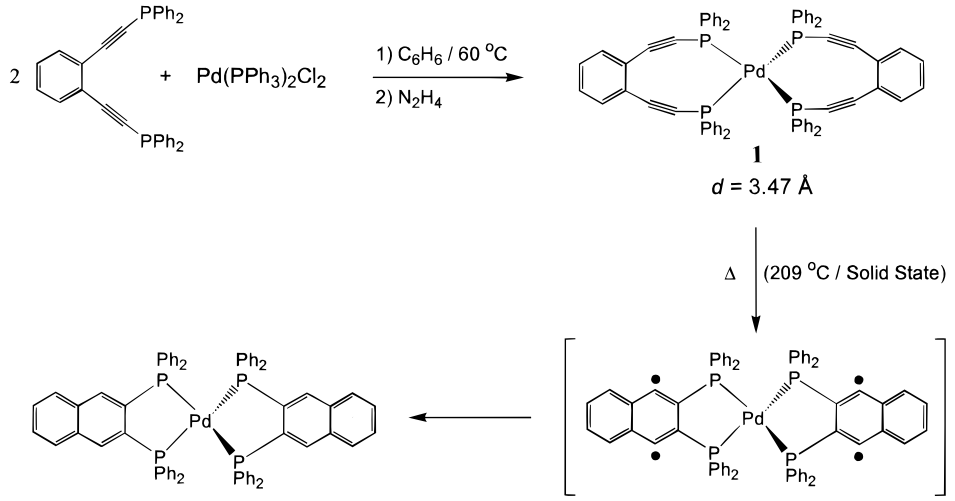

a triclinic cell. The choice of space group $P\bar{1}$ was later confirmed by the successful solution of the structure. Data processing produced a set of 9866 unique intensities and an $R_{av} = 0.029$ for the averaging of 3876 of these which had been measured more than once. The structure was solved using a combination of direct methods (MULTAN 78) and Fourier techniques. The position of the palladium atom was obtained from an initial E-map. The positions of the remaining non-hydrogen atoms were obtained from iterations of the least-squares refinement followed by a difference Fourier calculation. There was evidence in the difference maps for a molecule of CH_2Cl_2 solvent near a center of symmetry at 0, 0, 0 and another at $^3/_2$, $^1/_2$, 1. In addition, these atoms were disordered because of their close proximity to a symmetry element. Eventually, two half-weight molecules were included. Hydrogens were included in fixed calculated positions with thermal parameters fixed at one plus the isotropic thermal parameter for the parent carbon atom. In the final cycles of refinement, the non-hydrogen atoms for the Pd complex were varied with anisotropic thermal parameters that, with a scale and extinction parameter, gave a total of 659 variables. In the final difference map the largest peak was 1.8 e/Å^3, located 0.7 Å from Cl(77), and the deepest hole was −1.5 e/Å^3.

Crystallographic Structure Determination for 2. The single-crystal X-ray diffraction experiments were performed on a Siemens P4/CCD diffractometer for **2**. Systematic absences and diffraction symmetry are consistent for the space groups *P*1 and $P\bar{1}$. The *E*-statistics suggested the centrosymmetric option, which yielded chemically reasonable and computationally stable results of refinement. The structure was solved by the Patterson function, completed by subsequent difference Fourier syntheses, and refined by full-matrix, least-squares procedures. All non-hydrogen atoms were refined with anisotropic displacement coefficients. The CH_2Cl_2 solvate carbon atom is positionally disordered over an inversion center. Hydrogen atoms were treated as idealized contributions, except on the disordered carbon atom of the CH_2Cl_2 solvate which were ignored in the refinement but not in the global refinement parameters. All software and sources of the scattering factors are contained in the SHELXTL (5.10) program library (G. Sheldrick, Siemens XRD, Madison, WI).

Thermal Reactivity of 1 in Selected Solvents. A. *o*-Dichlorobenzene. An NMR tube was charged with 20 mg of $Pd(dppeb)_2$, 5 equiv of cyclohexadiene as H-donor, and 0.5 mL of *o*-dichlorobenzene. The sample was heated to 115 °C for 24 h followed by $^{31}P\{^1H\}$ NMR analysis. Identification of the reaction product as *trans*-Pd((2-chlorophenyl)diphenylphosphine)$_2Cl_2$ ($^{31}P\{^1H\}$ −5.1 ppm) (**2**) was made by obtaining crystals of the dibromide analog[49] via slow evaporation from CH_2Cl_2. The (2-chlorophenyl)diphenylphosphine ligand (**3**) was identified by mass spectrometry HMRS (FAB) *m*/*z* 296.1 (100) M^+ and $^{13}C\{^1H\}$ NMR ($CDCl_3$): δ 139.1 (d, 26.9 Hz), 136.9 (d, 11.9 Hz), 135.7 (d, 11.2 Hz), 133.9 (d, 21.7 Hz), 133.7 (d, 22 Hz), 129.9, 129.5, 129.0, 128.6 (d, 7.4 Hz), 128.4 (d, 7.3 Hz). Psuedo-first-order rate constants for the decay of **1** were obtained by integration of the $^{31}P\{^1H\}$ resonance at −5.6 ppm as a function of reaction time (*t*) and subsequently plotting of k_{obs} vs *t*. The activation energy for the decomposition of **1** was obtained from the slope of an Arrhenius plot of k_{obs} vs $1/T$ ($R^2 = 0.95$).

B. *o*-Fluorotoluene. Thermal activation of **1** in *o*-fluorotoluene was conducted according to the procedure described above in subsection A. At 115 °C the reaction went to completion within 24 h, while at lower temperatures, the reaction time increased from 2 to 7 days. The only products derive from decomposition of the starting compound which yielded unreacted dppeb ($^{31}P\{^1H\}$: δ −32.1 ppm).

Results and Discussion

Synthesis and Structure of 1. The dppeb ligand and the corresponding zerovalent $Pd(dppeb)_2$ compound were synthesized according to modified literature procedures.[50−52] Briefly, 2 equiv of the ligand were reacted with $Pd(PPh_3)_2Cl_2$ in benzene to produce **1** as an orange solid in 50% yield (Scheme 1). The compound is thermally stable (vide infra) and only mildly susceptible to air oxidation over a 24 h period in solution.

The structure of **1** features a tetrahedral Pd(0) center with four phosphorus atoms from two bound ligands that complete the coordination sphere (Table 1, Figure 2). The P−Pd−P bond angles nearly match the idealized 109.5° geometry expected for a d^{10} metal center in a tetrahedral ligand field (Table 2). The most important feature of the structure is the alkyne termini separation distance $d = 3.47$ Å. Although *d* is comparable in magnitude to the alkyne termini separation distance in the enediyne antitumor antibiotic dynemicin A triacetate ($d = 3.54$ Å)[53] and related synthetic analogues ($d = 3.6-3.7$ Å),[8,31] it is greatly reduced from the proposed free ligand distance of 4.1 Å.[45] Thus, the structure documents the ability of the metal to reduce the alkyne termini separation from that of the free ligand while maintaining the thermal stability of the uncyclized bis(chelate) for structure determination.

Several geometric characteristics observed in the structures of other enediyne motifs are also apparent in the structure of **1**. The first of these is the >12° deviation from linearity of the P−C≡C bond angles. The structure of dynemicin A triacetate

(49) Elemental analysis of **1** reveals trace amounts (0.23%) of Br^- ion although all reagents used in the synthesis, purification, and characterization were the chloride halo-form. The structure of **2** prompted elemental analyses of all reagents used in the preparation and subsequent thermal reactivity of **1**. Trace amounts of Br^- ion were indeed found in $PdCl_2$ (0.02%) and *o*-dichlorobenzene (0.05%) used despite the fact that all reagents were the highest purity commercially available.

(50) Warner, B. Personal Communication.

(51) McFarlane, H. C. E.; McFarlane, W. *Polyhedron* **1988**, *7*, 1875.

(52) Stern, E. W.; Maples, P. K. *J. Catal.* **1972**, *27*, 120.

(53) Konishi, M.; Ohkuma, H.; Tsuno, T.; Oki, T.; VanDuyne, G. D.; Clardy, J. *J. Am. Chem. Soc.* **1990**, *112*, 3715.

Table 1. Crystallographic Data for **1**

formula	$C_{69}H_{50}Cl_2P_4Pd$
formula weight	1180.38
color of crystal	yellow
crystal system	triclinic
space group	$P\bar{1}$
a, Å	13.326(5)
b, Å	21.332(8)
c, Å	11.601(4)
α, deg	105.72(1)
β, deg	115.88(1)
γ, deg	93.56(2)
V, Å^3	2793.42
Z	2
ρ_{calcd}, g/cm^3	1.403
T, K	105
λ, Å	0.71069
$R(F_o)^a$	0.070
$R_w(F_o)^b$	0.073

^{a} $R = \sum||F_o| - |F_c||/\sum|F_o|$. ^{b} $R_w = [\sum w(|F_o| - |F_c|)^2/\sum w|F_o|^2]^{1/2}$, where $w = 1/\sigma^2(|F_o|)$.

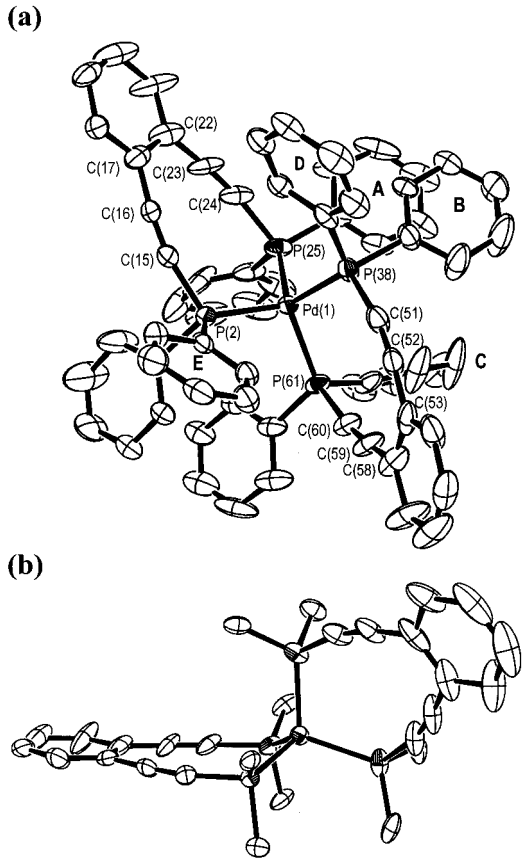

Figure 2. (a) ORTEP of the X-ray crystal structure of **1** (hydrogen atoms removed for clarity) as viewed down the 2-fold axis of a PdP_4 tetrahedron. Phenyl rings labeled A−E correspond to those with inter-ring closest contact interactions. (b) Thermal ellipsoid plot of **1** (phenyl rings removed for clarity) illustrating the planarity of the enediyne ligand and out-of-plane disposition (0.89 Å) of the Pd(0) center.

as well as those of biomimetic enediyne analogues also exhibit bending of the sp carbon that links the enediyne bridgehead to the remainder of the molecule. In general, angles ranging from 162 to 168° are observed in the structures of the antibiotic[53] and synthetic models,[31] suggesting that enediyne chelation to the metal in **1** qualitatively reproduces the geometric disposition of the alkyne termini within cyclic organic enediyne systems. Also noteworthy are the comparable deviations (∼10°) in the C≡C−C angles of the enediyne skeleton, which are once again

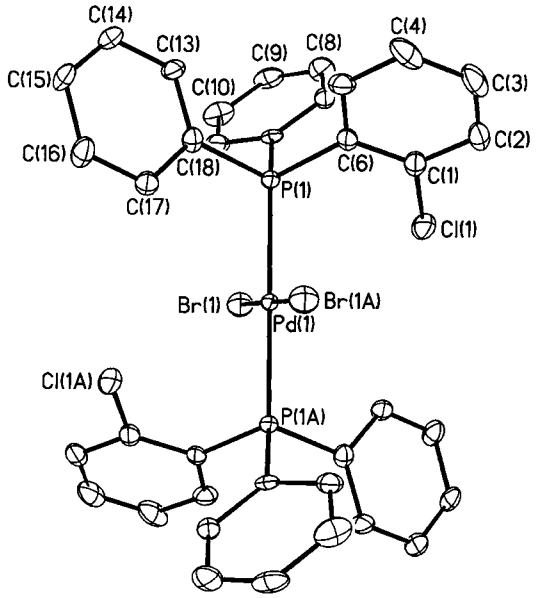

Figure 3. Thermal ellipsoid plot of **2** drawn at 30% probability. Hydrogen atoms and solvate molecules have been omitted for clarity.

Table 2. Selected Bond Distances (Å) and Angles (deg) for **1**

Pd−P(2)	2.3354(18)	C(15)−C(16)	1.195(8)
Pd−P(25)	2.3326(17)	C(23)−C(24)	1.175(9)
Pd−P(38)	2.3334(17)	C(51)−C(52)	1.197(9)
Pd−P(61)	2.3373(17)	C(59)−C(60)	1.206(8)
P(2)−Pd−P(25)	109.64(6)	P(25)−Pd−P(38)	110.99(6)
P(2)−Pd−P(38)	109.50(6)	P(25)−Pd−P(61)	109.42(6)
P(2)−Pd−P(61)	107.53(6)	P(38)−Pd−P(61)	109.69(7)
P(2)−C(15)−C(16)	166.9(6)	C(15)−C(16)−C(17)	169.4(8)
P(25)−C(24)−C(23)	167.7(6)	C(22)−C(23)−C(24)	171.5(7)
P(38)−C(51)−C(52)	167.3(6)	C(51)−C(52)−C(53)	171.7(7)
P(61)−C(60)−C(59)	167.6(6)	C(58)−C(59)−C(60)	169.0(8)

observed in the X-ray structure of dynemicin A triacetate (160−172°)[53] and synthetic analogues (169−173°).[8,31] Additionally, although some in-plane distortion of the enediyne ligand is apparent in the structure of **1**, the alkyne carbons within each ligand are nearly eclipsed revealing no out-of-plane bending in the molecule.

Ligand−ligand steric contributions to the structure of **1** are also evident in the X-ray diffraction analysis as two different interligand phenyl ring interactions are observed. The closest contact derives from a coplanar slipped *π*-stacking interaction at a 3.3 Å inter-ring separation between two phenyl groups (rings A and B in Figure 2) bound to phosphorus centers P25 and P38, respectively. Perpendicular to one of these partners (ring A) is an additional phenyl substituent (ring C) from a third phosphine (P61) of the PdP_4 tetrahedron at a 3.6 Å closest contact distance. Although these contributions to the structure of **1** are likely small, they do suggest the potential for using ligand−ligand steric interactions to influence the structure and thermal reactivities of metalloenediynes.

Thermal Reactivity of 1. Compound **1** is stable under ambient conditions and only reacts at significantly elevated temperatures. In the solid state, **1** exhibits a single exothermic phase transition at 209 °C ($\Delta H° = 54.7$ kcal/mol) consistent with the thermal cyclization of the enediyne ligands (Scheme 1).[45] No phase transition is detected in a second heating cycle following sample cooling to room temperature, indicative of an irreversible thermal reaction. In solution, **1** is stable at temperatures up to 100 °C over a 24 h period. Above this temperature, the compound readily decomposes to solvent-dependent products (Scheme 2). Heating of **1** in *o*-dichloroben-

Scheme 2. Thermal Reactivity of **1** in Solution

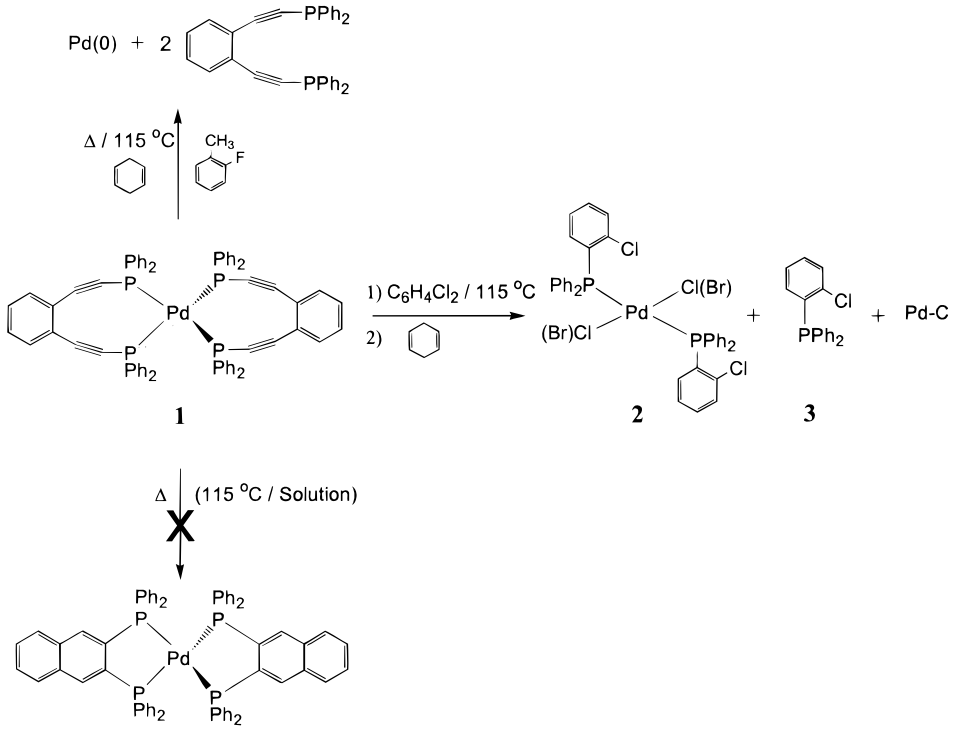

Table 3. Crystallographic Data for **2**

formula	$C_{37}H_{30}Br_2Cl_4P_2Pd$
formula weight	944.57
color of crystal	pale brown plock
crystal system	triclinic
space group	$P\bar{1}$
a, Å	9.4510(2)
b, Å	9.6419(2)
c, Å	11.6018(3)
α, deg	110.5270(9)
β, deg	109.0990(9)
γ, deg	98.4086(12)
V, Å^3	893.99(4)
Z, *Z*′	1, 1/2
ρ_{calcd}, g/cm^3	1.754
T, K	193
λ, Å	0.71069
$R(F)^a$	0.0827
$R(wF^2)^a$	0.2059

[a] Quantity minimized = $R(wF^2) = [\sum w(F_o^2 - F_c^2)/\sum(wF_o^2)^2]^{1/2}$; $R = \sum\Delta/\sum(F_o)$, $\Delta = |F_o - F_c|$ where $w = 1/[\sigma^2(F_o^2) + (aP)^2 + bP]$, $P = [2F_c^2 + \max(F_o, 0)]/3$.

Table 4. Selected Bond Distances (Å) and Angles (deg) for **2**

Pd−P(1)#1	2.350(2)	C(1)−C(2)	1.389(16)
Pd−Br(1)	2.4232(13)	C(2)−C(3)	1.39(2)
Pd−Cl(1)	3.416(4)	C(3)−C(4)	1.35(2)
P(1)−C(18)	1.822(10)	C(4)−C(5)	1.402(16)
P(1)−C(12)	1.847(9)	C(5)−C(6)	1.374(15)
P(1)−C(6)	1.838(10)		
P(1)#1−Pd(1)−P(1)	180.000(1)	C(18)−P(1)−C(6)	104.9(5)
P(1)#1−Pd(1)−Br(1)	88.08(7)	C(18)−P(1)−C(12)	102.1(4)
P(1)#1−Pd(1)−Br(1)#1	91.92(7)	C(12)−P(1)−C(6)	103.5(4)
Pd(1)−P(1)−C(18)	112.1(3)		
Pd(1)−P(1)−C(12)	120.5(3)		

zene at 115 °C for 2 h in the presence of cyclohexadiene (CHD) as an H-atom donor yields three products with $^{31}P\{^1H\}$ NMR resonances at −32.1, −10.6, and −5.1 ppm in a 1:3:1 ratio, respectively. The farthest upfield chemical shift corresponds to dissociation of uncyclized dppeb from **1**. The remaining oxidative addition product *trans*-Pd((2-chlorophenyl)diphenylphosphine)$_2$Cl$_2$ (**2**, −5.1 ppm), which has been identified by crystallographic characterization of the dibromide analogue (Tables 3 and 4),[49] and the corresponding free ligand (2-chlorophenyl)diphenylphosphine (**3**, −10.6 ppm),[54] derive from aryl−halide bond activation of the solvent. The mechanism responsible for the formation of these products is not clear[55] but may involve initial dissociation of dppeb from Pd(0) and subsequent oxidative addition of the phosphinoacetylide yielding phosphorus−carbon bond rupture. Within this framework, the resulting Pd(II) phosphide could then be stabilized by formation of a mixed-valence Pd(0,II) dinuclear complex in which the phosphide occupies a bridging position. Subsequent oxidative addition of the aryl−halide at the Pd(0) center generates a species in which the aryl halide and phosphide can reductively eliminate to give the uncomplexed compound **3**. In contrast to the solvent activation chemistry in *o*-dichlorobenzene, heating of **1** in the more robust solvent *o*-fluorotoluene at 115 °C for 2 h results in simple decomposition of **1** to yield uncyclized dppeb ($^{31}P\{^1H\}$ −32.1 ppm). No Bergman cyclization products are detected under these reaction conditions.

Structure/Reactivity Correlation. Comparison of the cyclization temperature for **1** with that of the previously reported Pd(dppeb)Cl$_2$ analogue reveals a striking dependence of the thermal barrier to cyclization on metal site geometry. The origin of this reactivity originates from two convoluted geometric factors: (1) the direct distance between the alkyne termini and (2) the ability of the metal center to adopt a planar transition state geometry leading to efficient Bergman cyclization. Experimental evidence for the first derives from thermal reactivity studies of dppeb with metal chlorides.[45] While the Hg^{2+} complex is reported to be unreactive due to a large alkyne termini separation (d = 3.4 Å), the solid state thermal reactivities of the Pd^{2+} and Pt^{2+} complexes show remarkable decreases in the cyclization temperatures of the bound dppeb relative to uncomplexed enediyne (DSC: Pd^{2+}, 61 °C; Pt^{2+}, 81 °C; dppeb, 243

(54) Grim, S. O.; Yankowsky, A. W. *Phosphorus Sulfur* **1977**, *3*, 191.
(55) Garrou, P. E. *Chem. Rev.* **1985**, *85*, 171.

°C). In solution, the Pd^{2+} complex has a half-life of 42 min at 35 °C, and the rate of cyclization can be measured at temperatures as low as 5 °C.[45] The facile reactivity of Pd(dppeb)Cl_2 is partially reflective of the 3.3 Å critical distance calculated for this compound, which compares favorably with organic analogues exhibiting similar distances and thermal cyclization temperatures.[7] Although crystallographic structure characterization of Pd(dppeb)Cl_2 has not been reported, the d^8 Pd^{2+} geometry is expected to be square planar with P−Pd−P angles close to 90°. In this case, the ligand field geometry of the metal center governs the disposition of the bound enediyne causing a reduction in the alkyne carbon termini separation and a consummate lowering of the thermal barrier to cyclization.

In addition to influencing the alkyne termini separation of the enediyne, evidence for the importance of the specific metal center geometry to cyclization reactivity can be obtained by comparison of activation energies for Bergman cyclization with theoretically determined transition state structures. The activation energy for Bergman cyclization of Pd(dppeb)$_2Cl_2$ has been determined experimentally to be a modest 12.3 kcal/mol.[45] For this process the dppeb ligand chelated to Pd can be viewed as a nine-membered metallocycle where the ligand field geometry of the metal center controls the P−Pd−P angle and consequently the alkyne termini separation distance. However, that is not the only structural influence the metal ion has on the enediyne unit. The geometry of the metal center also controls the overall planarity of the nine-membered ring. This is an important geometric consideration as density functional calculations for nine-membered carbocyclic enediynes have shown that the transition-state structure for Bergman cyclization possesses a planar ring geometry with a reduced alkyne termini separation (1.96 vs 2.91 Å).[56] The model suggests that the square-planar ground-state geometry of the Pd(II) center in Pd(dppeb)Cl_2 serves to more closely approach the transition state geometry required for facile Bergman cyclization, thereby contributing to the low thermal barrier to reactivity for this molecule.

Examination of the X-ray structure of **1** shows that the tetrahedral Pd(0) center is positioned 0.89 Å above the plane formed by the enediyne ligand (Figure 1b), making this system *geometrically* analogous to nine-membered carbocyclic enediynes. These organic compounds typically possess activation energies for Bergman cyclization from ∼10 to 30 kcal/mol depending upon the steric interactions between substituents on the three tetrahedral carbons closing the ring.[41] One of the prominent differences between the structures of the metallocycle and the carbocyclic enediynes is the elongated ring closing P−Pd−P bond distances (2.33 Å vs 1.4 Å) which partially relieve some of the steric interactions between the three adjacent tetrahedral centers. Based exclusively on this argument, **1** may be expected to exhibit a comparable or diminished activation barrier for Bergman cyclization relative to the carbocyclic enediyne analogues. Since **1** does not undergo Bergman cyclization in solution, an accurate measurement of the activation energy for this process is not possible. However, a lower limit can be estimated by determining the activation energy for the thermal decomposition of **1** in solution by NMR (Scheme 2). For this process, E_a has been determined to be 44 kcal/mol in *o*-dichlorobenzene by temperature-dependent rate constant measurements. The activation energy for Bergman cyclization of **1** in solution must therefore be > 44 kcal/mol, which is consistent with the enhanced alkyne termini separation and the resistance of the stable tetrahedral Pd(0) center to formation of a planar transition state that would favor Bergman cyclization. In relation to Pd(dppeb)$_2Cl_2$, this value is ∼30 kcal/mol more endothermic, and nearly 20 kcal/mol more endothermic than the nine-membered carbocyclic enediynes. Based on these results, we propose that the dramatic increase in the cyclization temperature of **1** relative to the dichloride analogue results directly from the increased alkyne termini distance in **1** (d = 3.47 Å vs 3.3 Å) caused by the increase in the P−Pd−P angle and the resistance of the ligand field stabilized tetrahedral Pd(0) geometry to bringing the alkyne carbons into close proximity for σ-bond formation in the transition state.[57]

Conclusion

Herein we report the unique X-ray crystal structure of a chelated metalloenediyne compound and its corresponding solid state and solution thermal reactivity. The tetrahedral geometry imposed by the d^{10} Pd(0) center forces the alkyne termini to a rigid separation distance of 3.47 Å. The ligand field stabilized geometry of the metal center also inhibits formation of a planar transition state that would bring the alkyne carbons into close proximity for σ-bond formation. As a result of these geometric influences, **1** is remarkably stable with no propensity to undergo Bergman cyclization. Our work demonstrates that metal binding can impose structural consequences upon the enediyne ligand governed by the ligand field mandated geometry of the metal center. The thermal reactivity of such systems can thus be modulated over a wide temperature range simply by judicious choice of metal−ligand geometry. Overall, this study provides conceptual insights into opportunities for modulating enediyne reactivity using transition metals and leads to considerable possibilities for designing novel metalloenediynes with potential biological utility.

Acknowledgment. We thank Drs. Mark Pagel and Ulrike Werner-Zwanziger of the Indiana University NMR Facility for technical assistance. The generous support of the American Cancer Society (RPG-99-156-01-C), the donors of the Petroleum Research Fund (PRF No. 33340-G4), administered by the American Chemical Society, and Research Corporation (Research Innovation Award No. RI0102 for J.M.Z) is gratefully acknowledged.

Supporting Information Available: Crystallographic data for **1** and **2** including tables of bond distances angles, final fractional coordinates and thermal parameters (PDF). This material is available free of charge via the Internet at http://pubs.acs.org.

JA9944094

(56) Koseki, S.; Fujimura, Y.; Hirama, M. *J. Phys. Chem. A* **1999**, *103*, 7672.

(57) It is impossible to rule out contributions to the activation energy for Bergman cyclization arising from steric clashes of the phenyl groups on adjacent ligands during progression to the transition state. However, sterically demanding tetrakis(diphenylphosphine) compounds of square-planar Pd(II) are synthetically established, and the X-ray structure of Pd-$[dppn]_2^{2+}$ documents the ability of four phenyl groups to adequately pack about a square-planar Pd(II) center (Oberhauser, W.; Backmann, C.; Stampfl, T.; Haid, R.; Brüggeller, P. *Polyhedron* **1997**, *16*, 2827). Moreover, since loss of dppeb is the initial step in the solution thermal reactivity of **1**, Bergman cyclized products arising from a Pd(0) monochelated intermediate might be expected to form if phenyl ring interactions were inhibiting the cyclization process at elevated solution temperatures. However, under these conditions no Bergman cyclization products are detected thereby suggesting that steric contributions from phenyl ring interactions are not the primary factor in determining the activation energy for the reactivity of **1**.